TRAJECTORY OPTIMIZATION FOR THE NATIONAL AEROSPACE PLANE

INTERIM
IN-05-CR
OCIT.
185663
14P

SEMI-ANNUAL REPORT

(December 13, 1992–June 12, 1993)

July, 1993

Research Supported by

NASA Langley Research Center

NASA Grant NO. NAG-1-1255

Technical Monitor: Dr. Daniel D. Moerder

Principal Investigator: Ping Lu

Department of Aerospace Engineering and Engineering Mechanics

Iowa State University

Ames, IA 50011

1. Introduction

During the past six months the research objectives outlined in the last semi-annual report [1] have been accomplished. Specifically, three-dimensional (3-D) fuel-optimal ascent trajectory of the aerospace plane and the effects of thrust vectoring control (TVC) on the fuel consumption and trajectory shaping have been investigated; the maximum abort landing area (footprint) has been studied; preliminary assessment of simultaneous design of the ascent trajectory and the vehicle configuration for the aerospace plane has also been conducted. An important goal of this research program is graduate student training. Mr. John Samsundar, a graduate student of Iowa State University, completed his Master of Science degree in Aerospace Engineering in May, 1993, under the support of this grant. His thesis is titled "An Investigation of Optimal Trajectories for an Aerospace Plane" [2]. Work under this grant has also produced a full length article in an archived journal during this period [3]. The following summarizes the work accomplished in the last six months. More detailed information can be found in [2–3].

2. Three-Dimensional Minimum-Fuel Ascent

So far all the research efforts on the study of minimum-fuel ascent trajectory of the aerospace plane have been exclusively in two-dimensional flight. The actual flight of the aerospace plane will not likely be restricted to 2-D flight, since some out-of-plane maneuvers may be required for given conditions at take-off and orbital insertion. It would be of great interest to understand how the out-of-plane maneuvers will influence the fuel consumption along the minimum-fuel trajectory, and whether or not the conclusions from study of 2-D flight will be valid for 3-D cases. While there is no more theoretical difficulty in 3-D flight than in 2-D case, the numerical difficulty is increased considerably because not only the number of state variables and controls in 3-D flight is increased, but also the inequality constraints on the trajectory are more difficult to satisfy. An inverse dynamics approach for trajectory optimization was developed in the first year of this research [3]. This approach

reduces the influence of poor conditioning typically associated with hypersonic trajectory optimization problems and has been very successful in 2-D trajectory optimization for the aerospace plane. It appears logical to continue to use this technique in 3-D flight.

The 3-D point-mass equations of motion for the aerospace plane over a spherical, nonrotating earth are

$$r' = \frac{r \tan\gamma \cos\phi}{\cos\psi} \tag{1}$$

$$\phi' = \tan\gamma \cos\phi \tag{2}$$

$$v' = (\frac{T\cos\alpha - D}{M} - \frac{\mu \sin\gamma}{r^2}) \frac{r\cos\phi}{v\cos\gamma\cos\psi} \tag{3}$$

$$\gamma' = (\frac{(T\sin\alpha + L)\cos\sigma}{mv} - (\frac{\mu}{vr^2} - \frac{v}{r})\cos\gamma) \frac{r\cos\phi}{v\cos\gamma\cos\psi} \tag{4}$$

$$\psi' = (\frac{(T\sin\alpha + L)\sin\sigma}{mv\cos\gamma} - \frac{v\cos\gamma\cos\psi\tan\phi}{r}) \frac{r\cos\phi}{v\cos\gamma\cos\psi} \tag{5}$$

$$m' = \frac{-T}{g_o I_{sp}} \frac{r\cos\phi}{v\cos\gamma\cos\psi} \tag{6}$$

where r is the radius from the center of the earth to the aerospace plane, ϕ latitude, v speed, γ flight path angle, ψ heading angle, and m mass. The independent variable is θ, the longitude. The prime denotes differentiation with respect to θ. The control variables are angle of attack α, bank angle σ, and fuel equivalence ratio Ω that influences the thrust T of the airbreathing engines and specific impulse I_{sp}. The idea of inverse dynamics is used as follows: Let $c(\theta)$ be a specified profile of the radius. Let

$$r(\theta) = c(\theta) \tag{7}$$

Differentiating Eq. (7) twice gives

$$\gamma' = \cos^2\gamma [\frac{\cos\psi}{r\cos\phi}(c'' - c'\tan\gamma) - \frac{c'}{r\cos^2\phi}(\psi'\cos\phi\sin\psi - \phi'\cos\psi\sin\phi)] \tag{8}$$

Using Eqs. (4) and (8) results in

$$L = \frac{mv}{cos\sigma}[\gamma' \frac{v\cos\gamma\cos\psi}{r\cos\phi} + (\frac{\mu}{vr^2} - \frac{v}{r})\cos\gamma - \frac{T\sin\alpha\cos\sigma}{mv}] \tag{9}$$

For given values of all the state variables, T, Ω and σ, Eq. (9) implicitly defines the required α to follow Eq. (7), which can be solved for numerically. Since this approach puts more direct control on the trajectory shaping by specifying r, the optimization process is more stable and much less sensitive to control variations. The problem is solved by parameterizing Ω, σ and r as functions of θ. The corresponding trajectory is obtained by numerically integrating the equations of motion. This way, the problem becomes a parameter optimization problem and a sequential quadratic programming (SQP) algorithm has been used to solve it [3].

The following initial and terminal conditions have been used in generating the solutions

$$\begin{aligned} r(0) &= R_0 \text{ radius of the earth} \\ \phi(0) &= 0 \\ v(0) &= 170\ m/s\ (Mach\ 0.5) \\ \gamma(0) &= 0 \\ \psi(0) &= 0 \\ m(0) &= 133,809\ kg\ (295,000\ lbf) \end{aligned} \tag{10}$$

$$\begin{aligned} r(t_f) &= R_o + 55\ km \\ \phi(t_f) &= 0^\circ,\ 5^\circ,\ 10^\circ,\ 15^\circ \\ v(t_f) &= 7839\ m/s \\ \gamma(t_f) &= 0 \\ \psi(t_f) &= free \end{aligned} \tag{11}$$

and an operational constraint

$$q \leq 95,760\ \text{N/m}^2\ (2000\ \text{psf}) \tag{12}$$

Figure 1 depicts the ascent trajectories for four cases. They almost coincide with each other. Other features of the 3-D trajectories also closely resemble those observed in 2-D cases [2–3]. The following table gives the time-of-flight and final mass for each of the trajectories.

Table 1: Time-of-flight and final mass for various final latitudes

ϕ_f(deg.)	t_f(sec.)	m_f(kg)
0	1311.2	67,112.0
5	1312.3	67,111.5
10	1312.5	67,111.1
15	1314.0	67,107.7

It is clear that there is practically no extra penalty on the fuel consumption for 3-D trajectories as compared to the 2-D case ($\phi_f = 0°$). The reason may become evident when one inspects Figs. 2 and 3 which show the histories of bank angle $\sigma(t)$ and latitude vs. longitude, respectively. It is seen that the vehicle only uses large bank angle in a short initial period to steer it into an appropriate plane and then remains approximately in planar motion thereafter. Figure 4 confirms this feature by showing the almost constant heading angle histories of the aerospace plane, after a quick initial change that aligns the vehicle in the right direction. Therefore for the most part, an optimal 3-D trajectory is in 2-D flight. Thus it may be concluded that the study of 2-D flight for the aerospace plane appears to be sufficiently representative of general motion in terms of fuel consumption and characteristics of the trajectory.

3. Abort Landing

As part of the investigation of the optimal trajectories for the aerospace plane, the capability of safe landing of the aerospace plane was assessed. The starting point is chosen to be a typical hypersonic cruise condition. Should any propulsion system failure develop at this point, the maximum reachable distances in all directions need to be known in order to explore all abort possibilities and determine an appropriate landing site. The trajectory optimization problem is also known as the footprint problem [4]. The formulation of the problem is as follows:

$$\text{maximize } \phi(t_f)$$

subject to the equations of motion Eqs. (1)–(5) with $T = 0$, initial conditions

$$\begin{aligned} r(0) &= R_0 + 30.5\ km \\ \phi(0) &= 0 \\ \theta &= 0 \\ v(0) &= 3351\ m/s\ (Mach\ 11) \\ \gamma(0) &= 0 \\ \psi(0) &= 0 \end{aligned} \tag{13}$$

(14)

and terminal conditions

$$\begin{aligned} r(t_f) &= R_o \\ \theta(t_f) &= \theta_f \\ v(t_f) &= 170\ m/s \\ \gamma(t_f) &= free \\ \psi(t_f) &= free \end{aligned} \tag{15}$$

When θ_f takes all possible values, the ground track of the point (θ_f, ϕ_f) represents the boundary of the maximum landing area (footprint). This is a 3-D trajectory optimization problem. The controls are the aerodynamic forces influenced by α and σ subject to $|\sigma| \leq 85°$. The problem is solved by directly parameterizing $\alpha(t)$ and $\sigma(t)$ and using the SQP algorithm. Figure 5 shows the footprint with the ground tracks of several trajectories. It is seen that that maximum downrange is about 2641 km and the maximum crossrange 1677 km. The minimum downrange is about -540 km (behind the starting point). The aerospace plane can glide to any landing site inside this footprint. Figure 6 illustrates some typical altitude profiles on the footprint. The oscillations in the altitude histories are characteristic of hypersonic optimal gliding trajectories [4]. The $\alpha(t)$ history for a typical trajectory is plotted in Fig. 7. We notice that the optimal α at each instant is approximately equal to

the value at which the lift-to-drag ratio C_L/C_D is maximized at that Mach number. This is also consistent with what previous researchers have observed [4]. Some bank angle histories are shown in Fig. 8.

4. Further Improvement on Fuel Efficiency

Because of the stringent flight path constraints and highly demanding orbital insertion conditions, the future aerospace plane is not likely to have any significant fuel margin. This part of the research aims at exploring various possibilities of further enhancing fuel efficiency of the aerospace plane.

4.1 Thrust Vectoring Control

The configuration of the aerospace plane (forebody as part of the compressor and aftbody as part of the nozzle) probably will make TVC difficult, and any TVC would be very limited if possible at all. However, from a trajectory analysis point of view, it would be interesting to have an assessment as how much more fuel could be saved should TVC is available. To this end, we allow a nonzero thrust angle ε to be used. The system equations are the same as Eqs. (1)–(6) except that the terms $\sin\alpha$ and $\cos\alpha$ in Eqs. (3)–(5) are replaced by $\sin(\alpha-\varepsilon)$ and $\cos(\alpha-\varepsilon)$. The study is restricted to 2-D flight. There are three control variables α, ε and Ω. Again, ε and Ω are parameterized directly and α solved using the inverse dynamic approach. The initial and terminal conditions are the 2-D versions of the conditions in Eqs. (10–11) with constraint (12) enforced. The objective is to find the minimum-fuel ascent trajectory.

Figure 9 shows the α and ε histories. With TVC, the final mass of the aerospace plane is 67,340 kg, comparing with 67,112 kg without TVC. The fuel saving by employing TVC is very small. This is because 75% of the optimal trajectory lies on the boundary of constraint (12). The fuel efficiency is already determined along that portion by the maximum allowable dynamic pressure (2000 psf). TVC can only improve the fuel efficiency in the short initial climbout and final zoom, which is rather limited. In conclusion, TVC does not appear to

offer significant improvement in fuel saving.

4.2 Simultaneous Design of Ascent Trajectory and Vehicle Configuration

Due to the unprecedented complexity of the aerospace plane, it has been well recognized that an integrated design approach that encompasses areas of propulsion, aerodynamics, structure and flight control is a necessity for the success of the vehicle. We believe that a simultaneous consideration of the design of the trajectory with vehicle design can also be quite beneficial in terms of further reducing the vehicle size and weight, because it has been found that there is a strong coupling between requirements on the trajectory and vehicle design specifications (e.g., the minimax dynamic pressure solution presented in Ref. [3]).

As a very preliminary study, we considered the trajectory optimization problem in which the control histories $\alpha(t)$ and $\Omega(t)$ (2-D case, no TVC) as well as the vehicle reference area S are to be optimized. S is chosen because it influences both aerodynamic lift, the main flight path control force, and the drag which a major fuel portion of the fuel is spent to overcome. The optimization yields a reference area of 82% of the value given in the original model [5]. The final mass is 68,986 kg, comparing with 67,112 kg with the reference area fixed at the original value. It should be stressed that this result is obtained by simplistically assuming that the change of S will not influence the aerodynamic coefficients of the aerospace plane. This, of course, is not realistic. Nonetheless, the result demonstrates the significant benefits that could be achieved by combining trajectory design with the vehicle configuration design.

References

[1] Lu, P., "Trajectory Optimization for the National AeroSpace Plane", Semi-annual report, NASA Grant NAG 1-1255, January, 1993.

[2] Samsundar, J., "An Investigation of Optimal Trajectories for an Aerospace Plane", M. S. Thesis, Iowa State University, May, 1993.

[3] Lu, P., "Inverse Dynamics Approach to Trajectory Optimization for an Aerospace

Plane", *Journal of Guidance, Control, and Dynamics*, Vol. 16, No. 4, July-August, 1993, pp. 726–732.

[4] Vinh, N. X., *Optimal Trajectories in Atmospheric Flight*, Elsevier Scientific Publishing Company, Amsterdam, The Netherlands, 1981

[5] Shaughnessy, J. D., Pinckey, S. Z., McMinn J. D., Cruz, C. I., and Kelley M-L., "Hypersonic Vehicle Simulation Model: Winged-Cone Configuration", NASA TM 102610, November 1990.

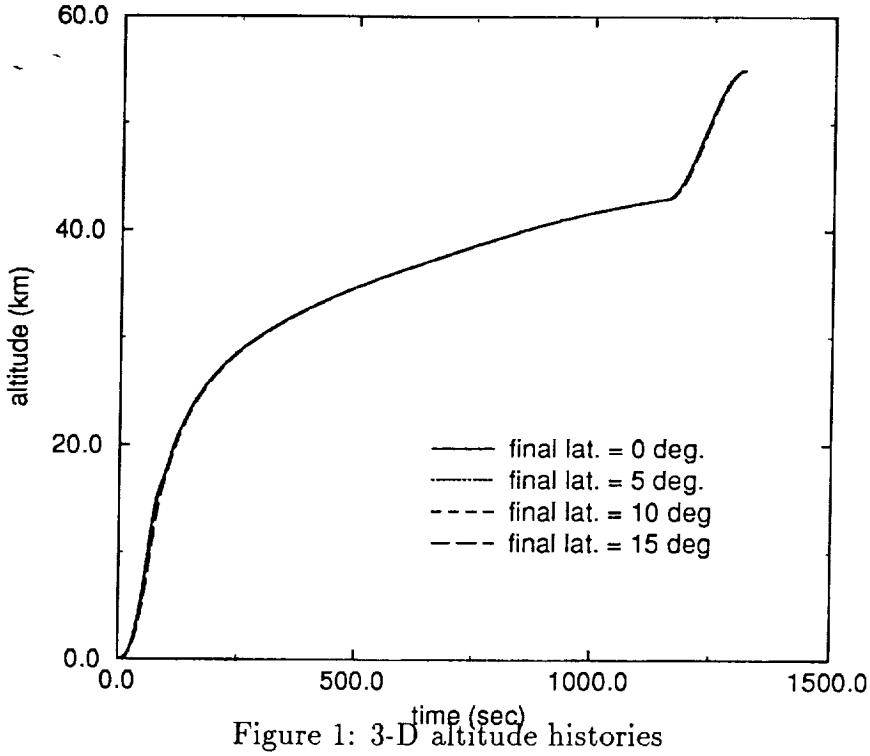

Figure 1: 3-D altitude histories

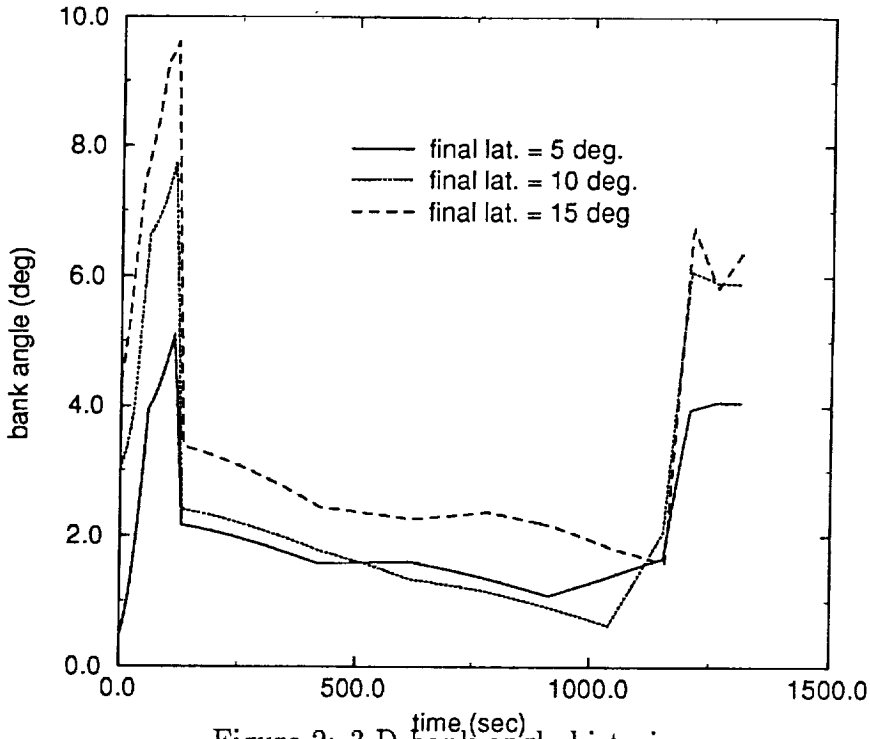

Figure 2: 3-D bank angle histories

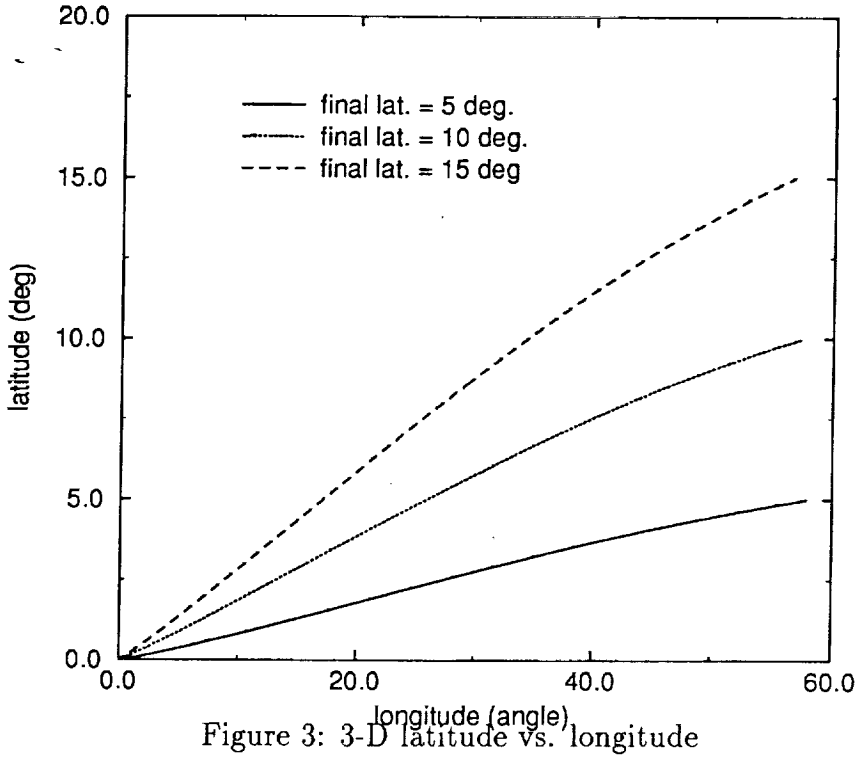

Figure 3: 3-D latitude vs. longitude

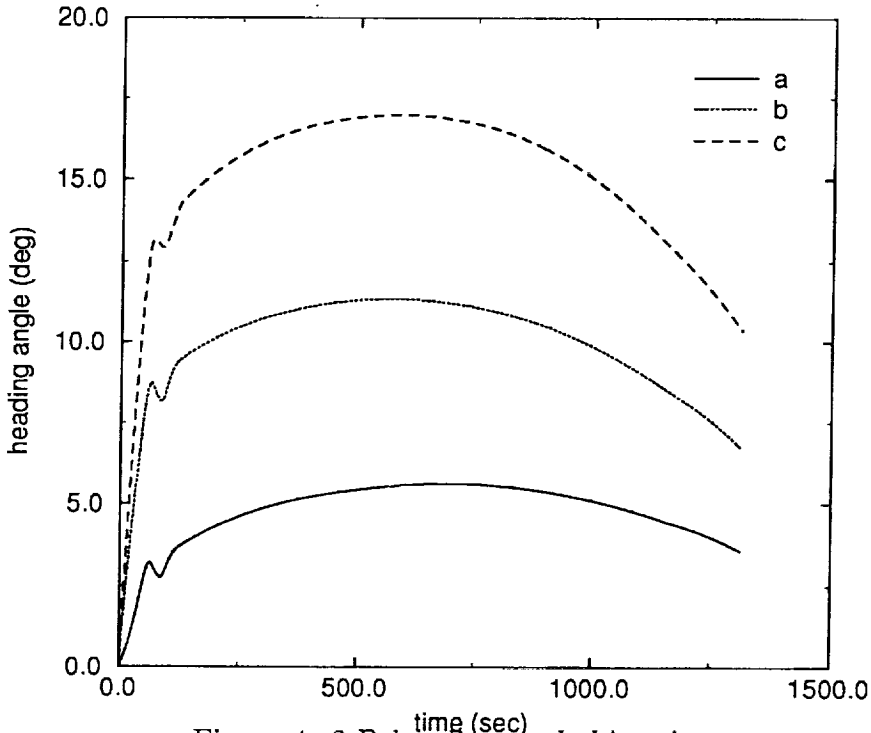

Figure 4: 3-D heading angle histories

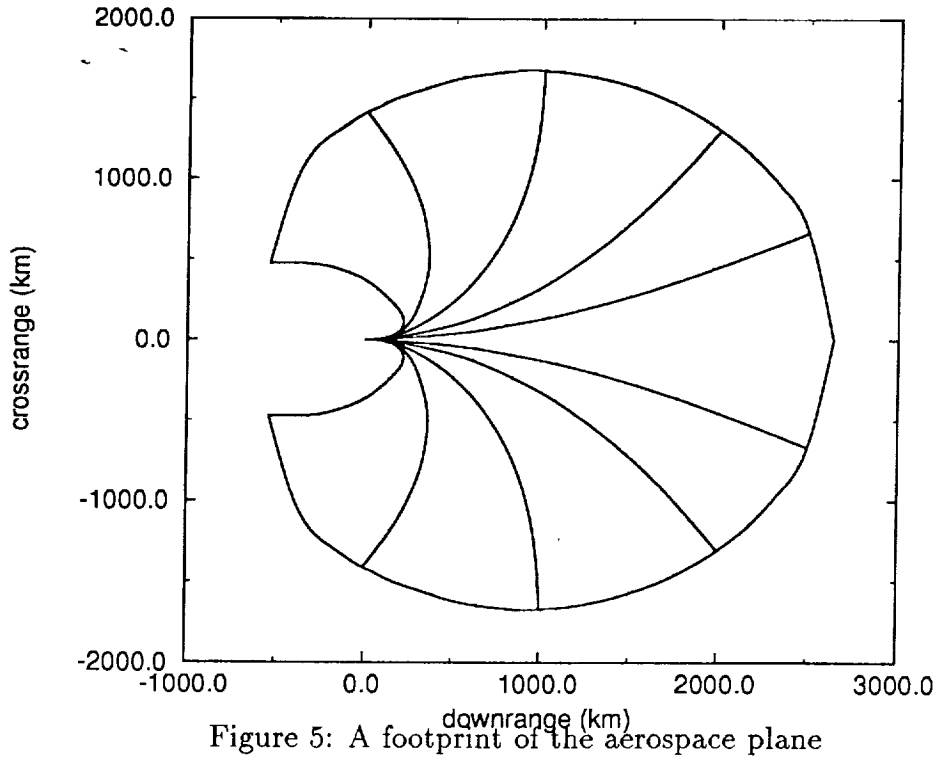

Figure 5: A footprint of the aerospace plane

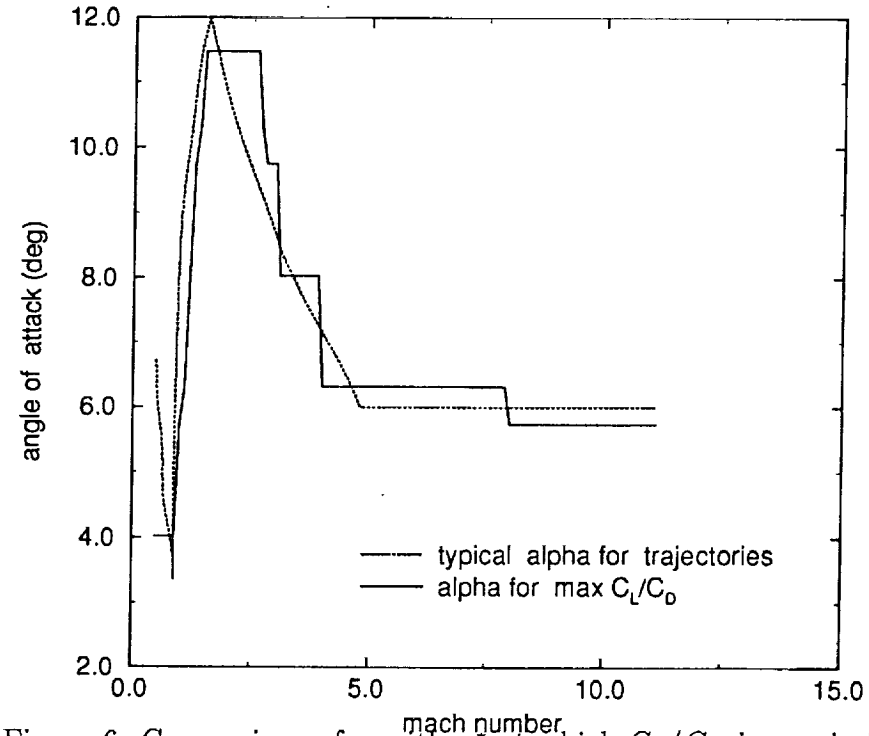

Figure 6: Comparison of α with α^* at which C_L/C_D is maximized

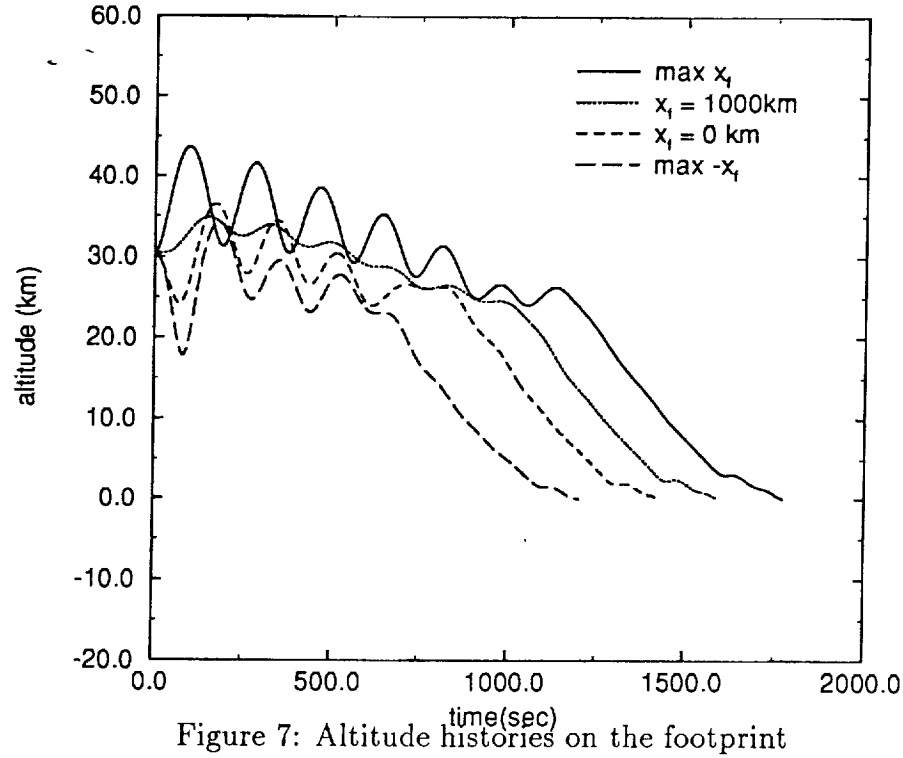

Figure 7: Altitude histories on the footprint

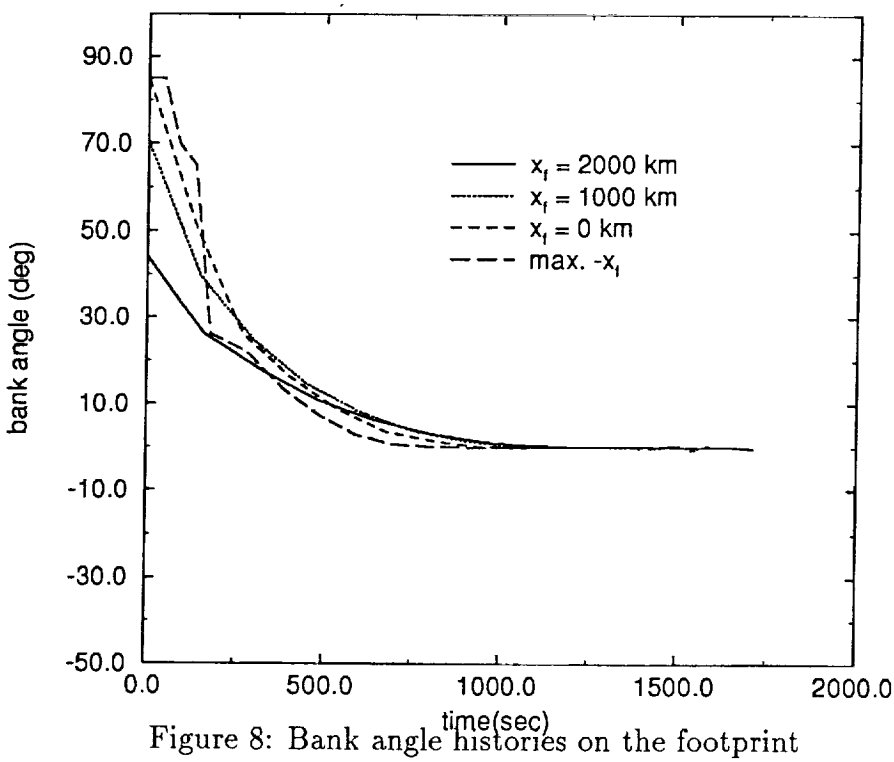

Figure 8: Bank angle histories on the footprint

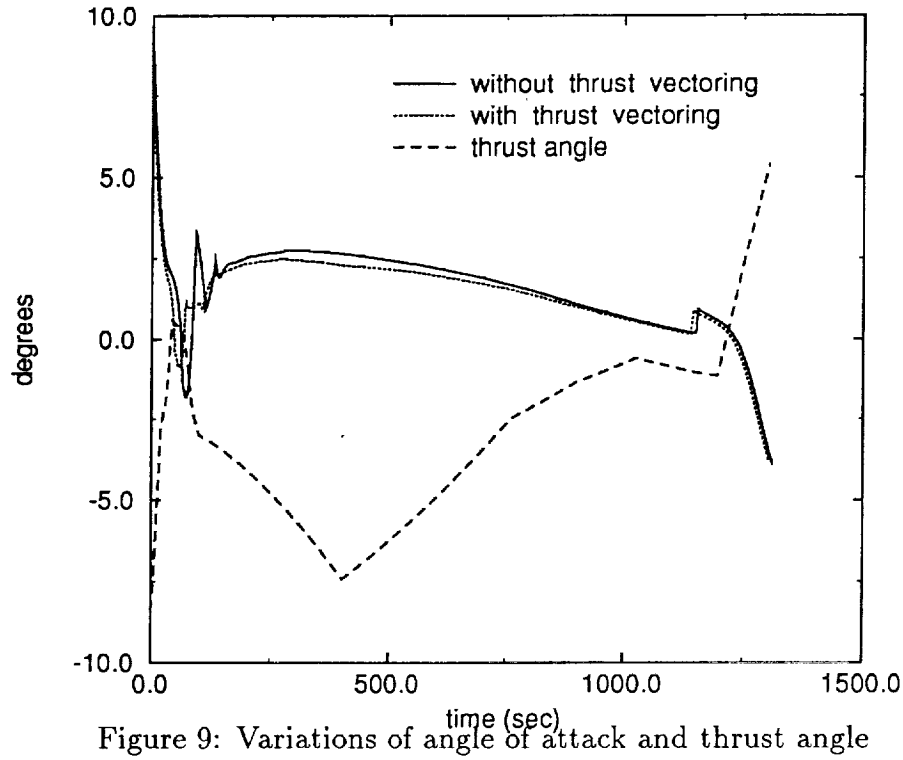

Figure 9: Variations of angle of attack and thrust angle